

Potassium Cation Effects on Site Preferences in the Mixed Cation Zeolite Li,Na–Chabazite

Luis J. Smith,^{†,§} Hellmut Eckert,^{*,‡} and Anthony K. Cheetham[†]

Materials Research Laboratory, University of California, Santa Barbara, California 93106,
and Institut für Physikalische Chemie, Westfälische Wilhelms-Universität Münster,
D-48149 Münster, Germany

Received August 7, 2000. Revised Manuscript Received November 1, 2000

The influence of potassium ions on the locations of Li⁺ and Na⁺ cations in dehydrated chabazites was studied by ⁷Li and ²³Na magic-angle spinning (MAS) nuclear magnetic resonance (NMR) spectroscopy and ²³Na multiple quantum MAS (MQMAS) NMR spectroscopy. ⁷Li MAS NMR reveals lithium chabazite to have two cationic sites: one at the six-ring window of the hexagonal prism (SII) and one in the supercage at the four-ring window of the hexagonal prism (SIII). Mixed lithium–sodium chabazites reveal strong evidence of selective occupancy for lithium cations accompanied by concomitant rearrangement effects. While the introduction of sodium and potassium into lithium chabazite reduces the Li site occupancies, no changes in lithium site preferences are observed: the SII site is favored over the SIII site. At low sodium content, sodium cations occupy a site in the eight-ring window of the channel (SIII') and at the center of the hexagonal prism (SI). In the presence of potassium, sodium cations reside at the SII sites vacated by the lithium cations at much lower sodium content than is observed in the lithium–sodium binary system. The introduction of potassium is associated with a marked increase in the lattice constant, resulting in the elimination of sodium cation site preferences.

Introduction

Lithium-containing faujasites and chabazites have demonstrated effective nitrogen sorption characteristics, making them useful in vacuum and pressure swing adsorption processes for air separation.¹ The separation effects are attributed to a strong interaction of the electric quadrupole moment of N₂ with the electrostatic field gradient created by the lithium cations.² Mixed cation forms of zeolites, containing both lithium and another cation, can impart greater thermal stability than fully lithiated forms while retaining the superior adsorption properties of lithium.¹ In these mixed forms of zeolites, the possibility exists for selective siting of the cations in various crystallographic positions. Accessibility of these extraframework cations will affect the sorption properties of the zeolite and, hence, manipulation of the site preferences of the cations can facilitate fine-tuning of the adsorption properties. For these reasons, recent work has been devoted to the structural characterization of the cation sites in mixed lithium–sodium forms of faujasite^{3,4} and chabazite.⁵

Zeolites of the chabazite family have a three-dimensional channel system that contains pores made from an eight-membered ring of oxygen atoms. The channel structure results from the connection of hexagonal prisms by four-membered ring units. Cation sites in dehydrated and hydrated forms of natural chabazite have been previously characterized.^{6–10} Three general cation positions are known to exist: one at the center of the prism (SI), one at the six-ring window of the prism (SII), and one at the eight-ring window (SIII, see Figure 1). With a pore size of 3.8 Å, chabazite is a useful material for separations dealing with the passage of small molecules such as N₂ and light olefins.

Past applications of both ⁷Li and ²³Na MAS NMR experiments to zeolites were able to identify distinct cation environments with varying degrees of resolution, despite the limited chemical shift ranges for the cationic forms of both nuclei. Previous work on mixed lithium–sodium chabazite showed a definite site preference for the cations in the dehydrated forms of the zeolite.⁵ Lithium cations are found to prefer coordination at the six-ring window (SII) of the hexagonal prism. Sodium

* To whom correspondence should be addressed.

[†] University of California.

[‡] Westfälische Wilhelms-Universität Münster.

[§] Current address: Department of Chemistry, Purdue University, 1393 Brown Laboratories, West Lafayette, IN, 47907-1393.

(1) Gaffney, T. R. *Curr. Opin. Solid State Mater. Sci.* **1996**, *1*, 69–75.

(2) Pápai, I.; Goursot, A.; Fajula, F.; Plee, D.; Weber, J. *J. Phys. Chem.* **1995**, *99*, 12925–12932.

(3) Feuerstein, M.; Lobo, R. F. *Chem. Mater.* **1998**, *10*, 2197–2204.

(4) Feuerstein, M.; Engelhardt, G.; McDaniel, P. L.; MacDougall, J. E.; Gaffney, T. R. *Microporous Mesoporous Mater.* **1998**, *26*, 27–35.

(5) Smith, L. J.; Eckert, H.; Cheetham, A. K. *J. Am. Chem. Soc.* **2000**, *122*, 1700–1708.

(6) Mortier, W. J.; Pluth, J. J.; Smith, J. V. *Mater. Res. Bull.* **1977**, *12*, 241–250.

(7) Mortier, W. J.; Pluth, J. J.; Smith, J. V. *Mater. Res. Bull.* **1977**, *12*, 97–102.

(8) Alberti, A.; Galli, E.; Vezzalini, G.; Passaglia, E.; Zanazzi, P. F. *Zeolites* **1982**, *2*, 303–309.

(9) Caligaris, M.; Mezzetti, A.; Nardin, G.; Randaccio, L. *Zeolites* **1984**, *4*, 323–328.

(10) Calligaris, M.; Mezzetti, A.; Nardin, G.; Randaccio, L. *Zeolites* **1986**, *6*, 137–141.

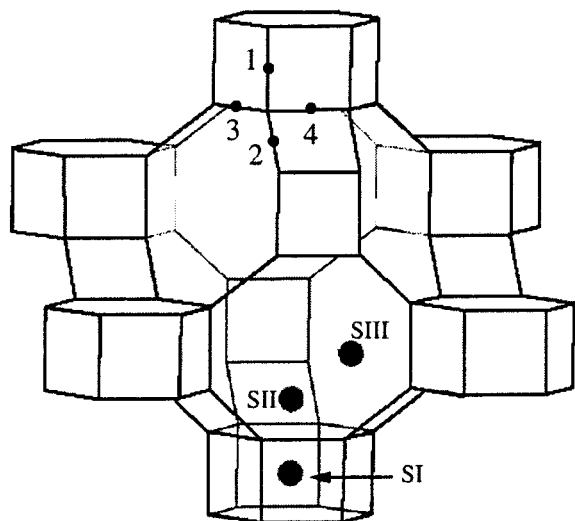


Figure 1. Representation of the extraframework cation positions in the hexagonal prism, SI, the six-ring window, SII, and the eight-ring window, SIII, of chabazite. The positions of the four unique oxygen atoms in the asymmetric unit are designated by atom number.

cations are preferentially directed toward the eight-ring window site (SIII) of chabazite, although occupation of the six-ring window does occur at higher sodium content.

In the ^7Li MAS NMR spectra of chabazite, typically weakly coordinated noncage lithium cations (such as those occupying the SIII site) have a lower resonance frequency than lithium coordinated in hexagonal prisms or six-membered rings. ^{23}Na MAS NMR distinguishes between cation environments but the trends are not always as clearly resolved as in ^7Li NMR. The broadened line shapes of ^{23}Na signals, due to coupling of the large nuclear electric quadrupole moment of sodium with the local electric field gradient of the cation environment, make the identification of individual sites rather difficult. Analysis of such spectra requires detailed line shape simulation and fitting procedures. The recently developed two-dimensional multiple-quantum magic-angle spinning (MQMAS) technique^{11,12} enables a line shape deconvolution into overlapping components based on differences in quadrupolar coupling and isotropic chemical shifts. Furthermore, this method allows site-resolved measurements of nuclear electric quadrupolar coupling constants. Because they reflect the local symmetries of individual cation environments, such coupling constants provide independent sources of structural information.

The characterization of the local cation environments and the site preferences in mixed lithium–sodium–potassium chabazites are the subject of this study. Owing to the size of the potassium cation, the extraframework site availability is more limited and thus its competition for the various sites is restricted. Nevertheless, indirect control over cation site preferences may occur through the effects of such a spectator cation on the zeolite lattice. To examine this possibility, ^7Li MAS, ^{23}Na MAS, and ^{23}Na MQMAS NMR spectra were

collected on a series of chabazite samples having variable sodium-to-lithium ratios and a fixed amount of potassium. Our results demonstrate that the site preferences of cations in these mixed-alkali chabazites can be altered by the presence of a small amount of a third species. Specifically, the presence of potassium in mixed lithium–sodium chabazites eliminates the site preferences normally exhibited by sodium in the binary system, resulting in sodium occupying all of the available extraframework cation sites.

Experimental Section

Sample Preparation and Characterization. The potassium form of chabazite was synthesized from the decomposition of the acid form of zeolite Y.¹³ The sodium form of zeolite Y was ion-exchanged with a 1 M NH_4Cl aqueous solution using a solution-to-zeolite ratio of 50 mL/g in four exchange cycles. The ammonium form was calcined at 450 °C in air to produce the acid form. The acid form of zeolite Y was then mixed with 6 M KOH and Ludox (LS-30) and placed in a 95 °C oven for 7 days.¹³ The resulting potassium chabazite was collected by filtration.

The as-synthesized zeolite was ion-exchanged to the mixed lithium–potassium form using 1 M LiCl aqueous solution at 100 °C at a solution-to-zeolite ratio of 50 mL/g in eight to ten exchange cycles, each lasting 6–8 h. The sodium form of chabazite was produced using the as-synthesized potassium chabazite in eight to ten ion-exchange cycles, each 6–8 h in duration using 1 M NaCl aqueous solutions, at the same solution-to-zeolite ratio. Following each ion-exchange step, the sample was collected via filtration and subsequently washed with deionized water using 2–3 times the ion-exchange volume. Mixed alkali forms of chabazite were produced by ion-exchanging stoichiometric amounts of the appropriate chloride solution with the conjugate 100% form of chabazite using only one exchange cycle. The actual cation ratios produced were verified through chemical analysis using inductively coupled plasma (ICP) spectroscopy. No significant cation deficiencies are evident within the error of the method. Five samples were produced having the following lithium, sodium, and potassium contents: 77% Li/23% K, 64% Li/13% Na/23% K, 53% Li/24% Na/23% K, 31% Li/47% Na/22% K, and 75% Na/25% K. The silicon-to-aluminum ratio for the precursor zeolite and various samples after ion exchange was determined to be 2.4 through both ICP and ^{29}Si NMR spectroscopy. All the zeolite samples were dehydrated under vacuum (5×10^{-5} Torr) at 500 °C and subsequently stored in an argon drybox where the samples were packed into MAS rotors for NMR experiments. ^{27}Al MAS NMR experiments were carried out on the dehydrated samples; no octahedral aluminum species were observed. X-ray diffraction patterns were collected on two mixed alkali samples: 77% Li/23% K chabazite and 75% Na/25% K chabazite at 295 K with a Scintag PAD-V powder diffractometer (45 kV, 35 mA) using Cu $K\alpha$ radiation. The diffraction pattern for the samples was analyzed using a cell constant determination routine provided with the Scintag software (Table 1).

NMR Spectroscopy. ^7Li and ^{23}Na NMR experiments were conducted on a Bruker Avance DSX-500 spectrometer with ^7Li and ^{23}Na resonance frequencies of 194.37 and 132.29 MHz, respectively. For both MAS and MQMAS experiments, a Bruker 4-mm high-speed MAS probe modified for providing extra-high B_1 -field amplitudes was used. One-dimensional ^7Li MAS spectra were acquired with a pulse length of 1.0 μs at a nutation frequency of 100 kHz for LiCl (aqueous). The spinning rate was 10 kHz and a recycle delay of 500 ms was employed. Under these conditions, rigorously quantitative spectra were recorded, allowing reliable site populations to be obtained. Chemical shifts are reported relative to a 1 M LiCl solution as a reference standard. The one-dimensional ^{23}Na MAS

(11) Frydman, L.; Harwood, J. S. *J. Am. Chem. Soc.* **1995**, *117*, 5367–5368.

(12) Medek, A.; Harwood, J. S.; Frydman, L. *J. Am. Chem. Soc.* **1995**, *117*, 12779–12787.

(13) Bourgogne, M.; Guth, J.-L.; Wey, R. U.S. Patent 4,503,024, 1985.

Table 1. Lattice Constants and Volumes of the Unit Cells for Mixed Li,K–Chabazite, Mixed Na,K–Chabazite, and Various Ratios of Mixed Li,Na–Chabazite

	<i>a</i> (Å)	α (deg)	vol (Å ³)	source
100% Li CHA	9.3357(5)	93.482(4)	808.7(7)	neutron ^a
76% Li/24% Na CHA	9.3369(15)	93.452(1)	809.1(4)	X-ray ^a
58% Li/42% Na CHA	9.3385(5)	93.382(4)	809.7(6)	neutron ^a
20% Li/80% Na CHA	9.3423(41)	92.694(1)	812.4(11)	X-ray ^a
9% Li/91% Na CHA	9.3536(33)	92.731(1)	815.2(9)	X-ray ^a
100% Na CHA	9.3716 (10)	92.643(1)	820.2(3)	neutron ^a
75% Na/25% K CHA	9.4077(87)	92.2663(4)	830(2)	X-ray
77% Li/23% K CHA	9.4262(41)	92.1032(1)	836(1)	X-ray

^a From ref 5.

experiments were performed at a spinning speed of 12 kHz using a 0.5- μ s pulse at a nutation frequency of 100 kHz for NaCl (aq) with a recycle delay of 500 ms for all samples. The MAS spectra were fitted using the deconvolution routine from the xedplot program in the XWIN-NMR suite of programs for the Bruker spectrometer. The intensities for the fit of the second-order quadrupolar broadened lines were adjusted according to the procedure described by Massiot et al.¹⁴ to account for spinning sideband intensity not included in the MAS centerband. In the present samples, the procedure is indispensable for obtaining correct cation populations in the spectra.

The two-dimensional ²³Na MQMAS experiments were carried out using the three-pulse zero-quantum filter sequence developed by Amoureux and co-workers.¹⁵ The first and second pulses were hard pulses using a nutation frequency of 250 kHz for NaCl (aq) and had pulse lengths of 2 and 0.8 μ s, respectively. The third pulse was a soft 90° pulse of 8.4 μ s in length (nutation frequency of 32 kHz). The increments of the t_1 period, the delay between the first and second pulse, were typically 5 μ s. A fixed delay of 10 μ s was used between the second and third pulse. The spectra were typically collected with 64–128 different t_1 periods. Signals from the echo and antiecho were separated using the States method.¹⁶ A recycle delay of 500 ms was employed and 800–1400 scans were collected per row. The resulting two-dimensional data set was Fourier-transformed and sheared according to the method described by Massiot et al.¹⁷ However, in addition to scaling the dwell time in the F_1 (isotropic) dimension and the offset in the isotropic dimension, the spectrometer frequency in the isotropic dimension was multiplied by the factor $(k + 3)/(1 + k)$.¹⁸ For quadrupolar nuclei with a spin of 3/2, k has a value of 7/9. Scaling the isotropic dimension in this fashion serves to separate distributions in the chemical shifts and quadrupolar couplings by distinct slopes in the transformed spectra. All the ²³Na chemical shifts are reported relative to a 1 M aqueous NaCl solution reference standard.

Isotropic chemical shift and quadrupolar product ($P_q = C_Q(1 + \eta^2/3)^{1/2}$) information can be obtained from these MQMAS spectra. Here, C_Q and η denote the ²³Na nuclear electric quadrupolar coupling constant (in MHz) and the asymmetry parameter, respectively. The peaks in the MQMAS spectra have positions based on the following relationships,

$$\delta_{F_1} = \delta_{cs} + \frac{P_q^2 \times 10^6}{68\nu_0^2} \quad (1)$$

$$\delta_{F_2} = \delta_{cs} - \frac{P_q^2 \times 10^6}{40\nu_0^2} \quad (2)$$

where ν_0 is the ²³Na Larmor frequency (in MHz) of an isotropic sample.

The first moment of the peak in the second dimension is used because the fourth-ranked terms are zero at the center of mass of the line.¹² From these equations, it is clear that distributions of isotropic chemical shifts with a similar quadrupolar product will have a slope of 1 in the two-dimensional contour plot. Distributions of the quadrupolar product for

resonances with the same or similar isotropic chemical shifts will have a slope of $-10/17$. The isotropic chemical shift and quadrupolar product are calculated using the following relationships:

$$\delta_{cs} = \frac{10}{27}\langle\delta_{F_2}\rangle + \frac{17}{27}\langle\delta_{F_1}\rangle \quad (3)$$

$$P_q = \sqrt{\frac{680\nu_0^2 \times 10^{-6}}{27}(\langle\delta_{F_1}\rangle - \langle\delta_{F_2}\rangle)} \quad (4)$$

Results

Figure 2 summarizes the ⁷Li and ²³Na NMR data obtained for the whole suite of samples. Table 2 summarizes the chemical shifts and lithium site populations deduced from ⁷Li NMR. The ⁷Li MAS NMR spectrum of the 77% Li/23% K chabazite consists of two peaks at -0.23 and -0.68 ppm. Previous ⁷Li NMR studies of 100% lithium chabazite assigned the higher frequency peak to the SII site. From this assignment and the accompanying populations, it is clear from Table 2 that the majority of potassium replaces lithium at the SIII site. With increasing sodium content, the population of Li in both sites decreases. However, the lower frequency peak, assigned to the SIII site, diminishes at a higher rate and disappears before the complete replacement of lithium with sodium.

The ²³Na MAS NMR spectra exhibit a complex line shape that is the result of the overlap of the anisotropic NMR signals from numerous sodium sites. The ²³Na MQMAS spectra in Figure 3 resolve much of the overlap encountered in the one-dimensional MAS spectra. The δ_{iso} and P_q values extracted from these spectra are collected in Table 3. The introduction of sodium into the mixed lithium–potassium chabazite initially results in only one type of sodium environment, as shown in Figure 3a. The chemical shift and quadrupolar product for this site are consistent with a sodium cation in the SIII' site.⁵ Exchanging lithium cations for sodium cations up to 24% sodium content increases the number of environments observable to five, as evidenced in Figure 3b. The values of the isotropic chemical shifts and quadrupolar products for the five sites are typical for sodium cations in SI-, SII-, and SIII'-type cation sites. Two SIII' sites are observable; while one of them, SIII'a, is identical to the one observed at the lowest Na content, the other one, SIII'b, is characterized by a wide chemical shift distribution due to disorder, similar to that observed in mixed sodium–lithium chabazite.⁵ This chemical shift distribution is evidenced by the characteristic sloping of the signal in the two-dimensional plot (see above). In contrast to the binary Li–Na chabazite system, we also observe two SII-type environments in the present samples, characterized by slightly different chemical shifts and quadrupolar products. Finally,

(14) Massiot, D.; Bessada, C.; Coutures, J. P.; Taulelle, F. *J. Magn. Reson.* **1990**, *90*, 231–242.

(15) Amoureux, J.-P.; Fernandez, C.; Steuernagel, S. *J. Magn. Reson. A* **1996**, *123*, 116–118.

(16) Ernst, R. R.; Bodenhausen, G.; Wokaun, A. *Principles of Nuclear Magnetic Resonance in One and Two Dimensions*; Clarendon: Oxford, 1987.

(17) Massiot, D.; Touzo, B.; Trumeau, D.; Coutures, J. P.; Virlet, J.; Florian, P.; Grandinetti, P. *J. Solid State Nucl. Magn. Reson.* **1996**, *6*, 73–83.

(18) Fernandez, C.; Amoureux, J. P.; Chezeau, J. M.; Delmotte, L.; Kessler, H. *Microporous Mater.* **1996**, *6*, 331–340.

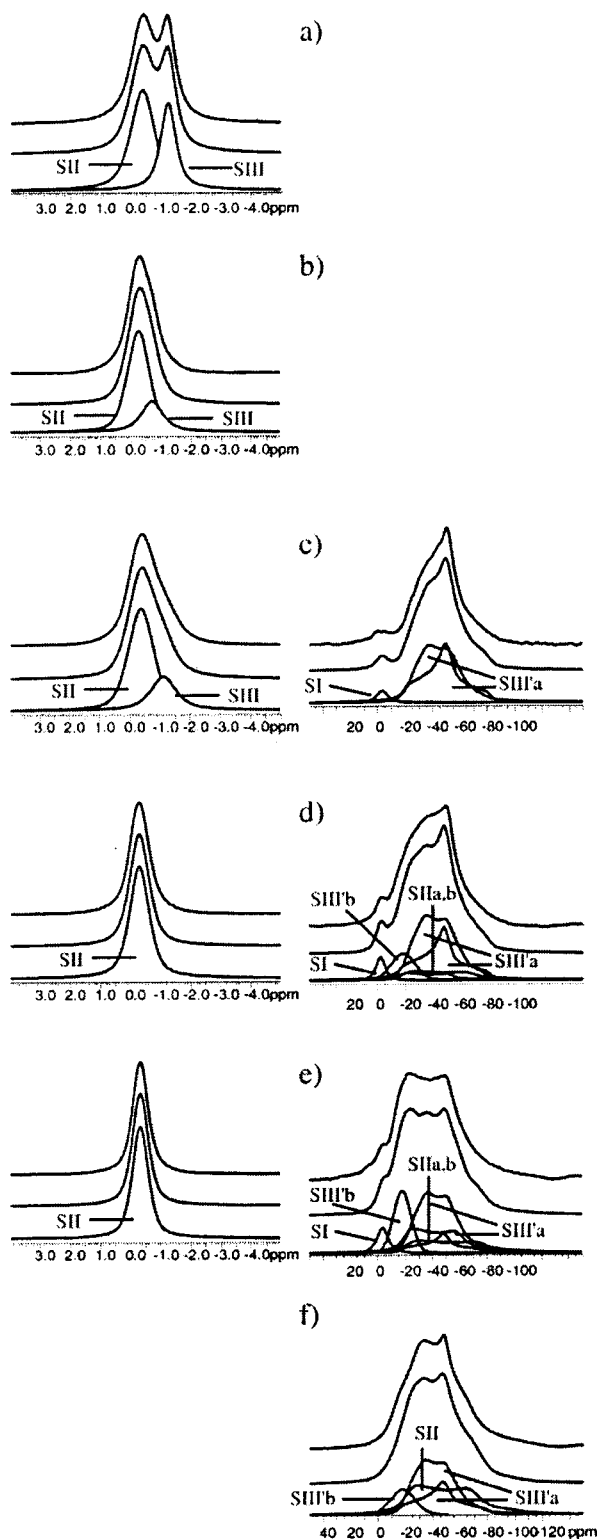


Figure 2. ^7Li MAS NMR (left) and ^{23}Na MAS NMR (right) spectra of chabazite with the various cation contents: (a) 100% Li (reproduced with permission from ref 5), (b) 77% Li/23% K, (c) 64% Li/13% Na/23% K, (d) 53% Li/24% Na/23% K, (e) 31% Li/47% Na/22% K, and (f) 75% Na/25% K. The experimental spectrum is shown in the upper trace, the simulated in the middle, and the components of the simulation at the bottom.

assignment of the SI-type site is based on its chemical shift and small quadrupolar product; values similar to these have been observed for sodium in faujasite, which also has an SI-type site available for cations.^{4,19} Increasing the sodium cation content to higher levels (47%,

Table 2. ^7Li NMR Chemical Shifts (± 0.05 ppm) and Site Populations of Li-Containing Chabazite Samples

	SII	SIII	total
100% Li ^a			
δ_{iso} (ppm)	-0.37	-1.22	
Li ⁺ /u.c.	2.22	1.31	3.53
77% Li/23% K			
δ_{iso} (ppm)	-0.23	-0.68	
Li ⁺ /u.c.	2.01	0.71	2.72
64% Li/13% Na/23% K			
δ_{iso} (ppm)	-0.34	-1.08	
Li ⁺ /u.c.	1.63	0.63	2.26
53% Li/24% Na/23% K			
δ_{iso} (ppm)	-0.27		
Li ⁺ /u.c.	1.87	0	1.87
31% Li/47% Na/22% K			
δ_{iso} (ppm)	-0.29		
Li ⁺ /u.c.	1.09	0	1.09

^a From ref 5.

Figure 3c) does not increase the number of observable environments but does affect the relative site populations. Total replacement of the lithium cations by sodium results in a drastic change in the MQMAS spectra, as shown in Figure 3d, with the number of environments decreasing and the resulting spectra resembling the results for 100% sodium chabazites.

To determine the populations of the different environments, the spectral parameters deduced from the MQMAS spectra were used as starting points for simulating the ^{23}Na MAS spectra in Figure 2. The simulation parameters and population data extracted in this way are summarized in Table 4.

As was the case for the binary system, simulation of the ^{23}Na MAS NMR line shape for the SIII'a site in the 13% sodium chabazite (and in the other samples as well) required the use of two quadrupolar broadened spectral components. The two components have similar chemical shifts and quadrupolar coupling constants but different asymmetry parameters, η , of 0.4 and 1.0. The SIII'a site probably has a distribution in the asymmetry of the electric field gradient due to the aluminum disorder in the tetrahedral sites and the resulting effect on the partial charges of the oxygen atoms in the framework. Nevertheless, two spectral components were sufficient to simulate the line shape. Analogous to the binary system, the line shape of the disordered SIII'b site observed at Na content > 13% was simulated using a broad Gaussian curve to reflect the chemical shift distribution present for that site.

A comparison of Tables 3 and 4 indicates some systematic differences between the spectral parameters extracted for each site from the MQMAS data and those obtained from the refined fits of the MAS NMR data. We have noted similar discrepancies in the binary system and attribute them to an artifact arising from nonuniform excitation of the triple-quantum transitions in conjunction with distributions of spectral parameters. Despite this complication, the data obtained from the refinement of the MAS NMR data allow a consistent discussion of the compositional effects observed in the present suite of samples studied.

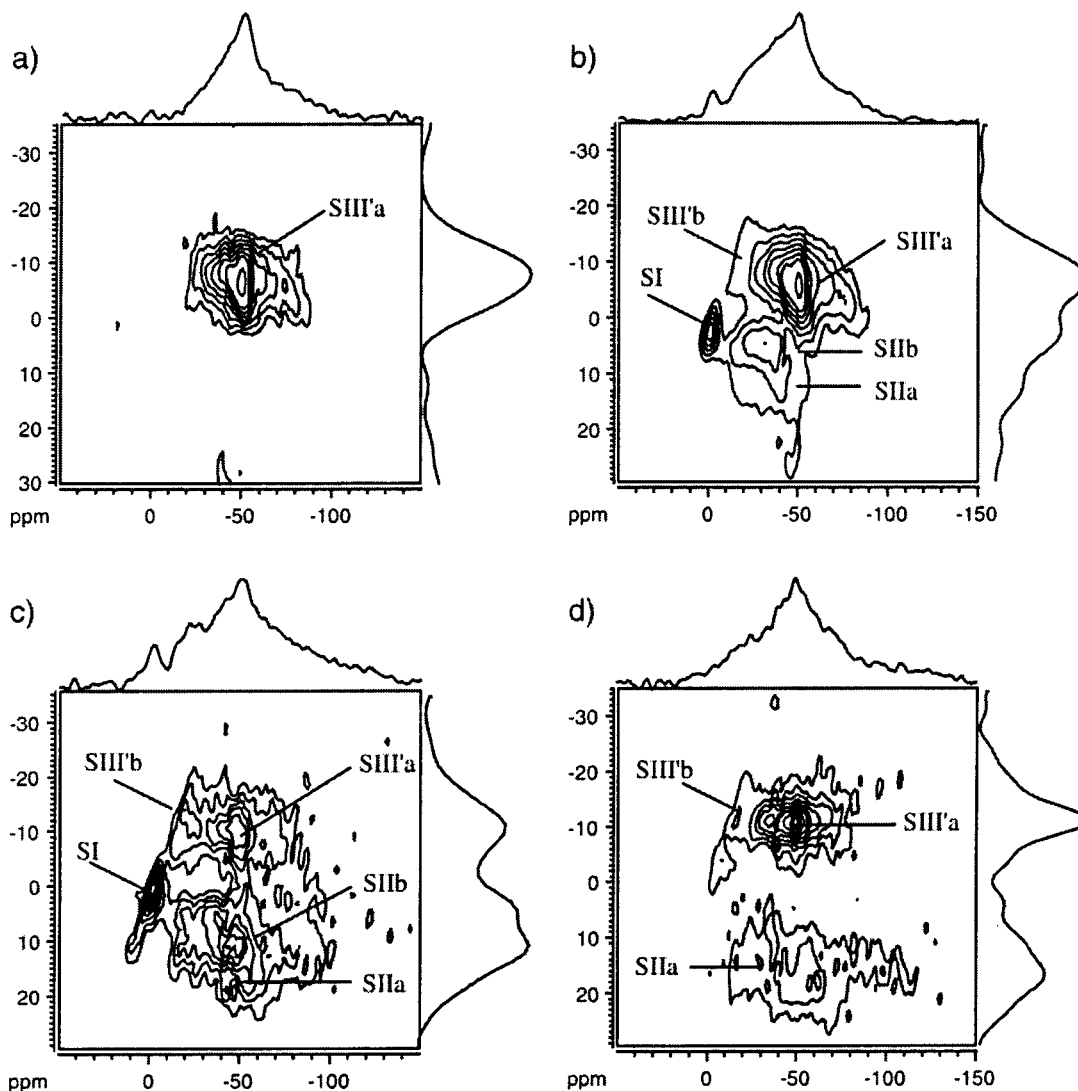


Figure 3. ^{23}Na MQMAS NMR spectra for (a) 64% Li/13% Na/23% K chabazite, (b) 53% Li/24% Na/23% K chabazite, (c) 31% Li/47% Na/22% K chabazite, and (d) 75% Na/25% K chabazite. The projection of the anisotropic MAS dimension is at the top; the projection of the isotropic dimension is to the right. The different sodium sites are identified in the spectra.

Table 3. Isotropic Chemical Shift and Quadrupolar Coupling Data from ^{23}Na MQMAS Spectra

	SIII'a	SIII'b	SI	SIIa	SIIb
75% Na/25% K					
δ_{iso} (ppm)	-24.7 ± 1.5	-10.0 ± 1 to -22.8 ± 1^a		-15.3 ± 1.5	
P_q (MHz)	4.1 ± 0.1	1.7 ± 0.2		5.7 ± 0.1	
31% Li/47% Na/22% K					
δ_{iso} (ppm)	-25 ± 3	-11.0 ± 1 to -21.0 ± 1^a	-1 ± 3	-14 ± 3	-12 ± 3
P_q (MHz)	4.1 ± 0.2	2.0 ± 0.2	1.2 ± 0.7	4.9 ± 0.2	5.3 ± 0.2
53% Li/24% Na/23% K					
δ_{iso} (ppm)	-22 ± 2	-11.0 ± 1 to -20.3 ± 1^a	1 ± 2	-12 ± 2	-10 ± 2
P_q (MHz)	4.3 ± 0.2	2.0 ± 0.2	1.3 ± 0.5	4.4 ± 0.2	5.1 ± 0.1
64% Li/13% Na/23% K					
δ_{iso} (ppm)	-23 ± 2				
P_q (MHz)	4.4 ± 0.2				

^a Range of chemical shifts; see text.

Discussion

Figures 4 and 5 show the lithium and the sodium site occupancies as a function of the combined $\text{Na}^+ + \text{K}^+$ fraction. Qualitatively, the trends exhibited in these occupancies are similar to those observed in the binary Li–Na–chabazite; however, some important differences can be noted as well. Lithium occupation of the SII site remains saturated with the initial introduction of cations at the SIII' sites. The ^7Li NMR spectrum of the

Li–K chabazite demonstrates clearly that the potassium ions reside primarily at the SIII' site. For the ternary Li–Na–K samples, the trend for lithium occupation of the SII and SIII sites is very similar to that observed in the binary Li–Na system, as shown in Figure 4. We thus conclude that the introduction of potassium does not affect the lithium site preferences.

For the sodium occupancies, interesting differences emerge in comparison to binary Na,Li–chabazites. As

Table 4. ^{23}Na MAS NMR Simulation Parameters and Site Populations of the Various Mixed Na,Li,K-Chabazites

	SIII'a	SIII'a	SIII'b ^a	SI	SIIa	SIIb	total
75% Na/25% K							
δ_{iso} (ppm)	-15.7 ± 1.0	-19.7 ± 1.0	$-12.0, \sigma = 8.9$		-8.7 ± 1.0		
C_Q (MHz)	4.0 ± 0.2	4.0 ± 0.2	2.0		5.3 ± 0.2		
η	1.0	0.4			0.1		
Na ⁺ /u.c	0.35	0.61	0.14		1.54		2.64
31% Li/47% Na/22% K							
δ_{iso} (ppm)	-16.9 ± 1.0	-19.9 ± 1.0	$-11.6, \sigma = 7.5$	-0.50 ± 1.0	-10.0 ± 1.0	-8.6 ± 1.0	
C_Q (MHz)	3.9 ± 0.2	3.9 ± 0.2	2.0	1.3 ± 0.2	4.7 ± 0.2	5.4 ± 0.2	
η	1.0	0.4		0.1	0.1	0.1	
Na ⁺ /u.c	0.15	0.50	0.14	0.05	0.38	0.45	1.67
53% Li/24% Na/23% K							
δ_{iso} (ppm)	-15.3 ± 1.0	-18.3 ± 1.0	$-12.6, \sigma = 10.1$	0.59 ± 1.0	-8.3 ± 1.0	-7.3 ± 1.0	
C_Q (MHz)	4.0 ± 0.2	4.0 ± 0.2	2.0	1.3 ± 0.1	4.4 ± 0.2	5.2 ± 0.2	
η	1.0	0.4		0.1	0.1	0.1	
Na ⁺ /u.c	0.25	0.31	0.06	0.02	0.04	0.17	0.85
64% Li/13% Na/23% K							
δ_{iso} (ppm)	-17.7 ± 1.0	-20.9 ± 1.0		-0.31 ± 1.0			
C_Q (MHz)	3.9 ± 0.2	3.4 ± 0.3		1.3 ± 0.1			
η	1.0	0.4		0.1			
Na ⁺ /u.c	0.23	0.22		0.01			0.46

^a σ equals full-width at half-maximum for chemical shift distribution; see text.

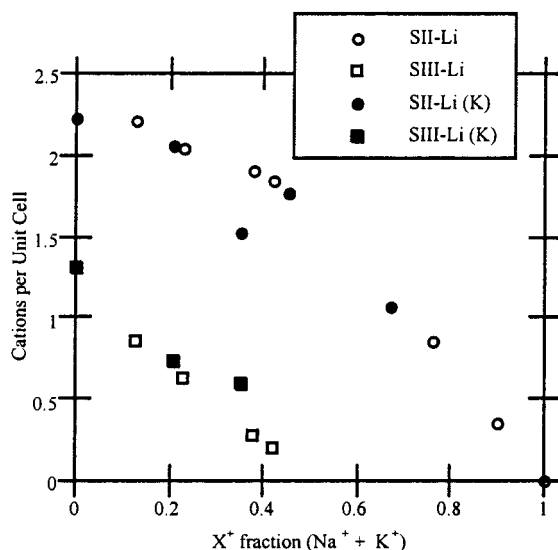


Figure 4. Plot of the lithium occupancies in mixed alkali chabazite with (filled symbols) and without (open symbols) the presence of potassium, as a function of the combined fraction (X^+) of sodium and potassium ions. The lithium occupancy data from the Li,Na-chabazite is reproduced with permission from ref 5.

in the binary system, sodium first occupies the SIII' site up to a threshold concentration above which the SII site is also occupied. However, this threshold concentration is significantly lowered by the presence of potassium in the present samples: SII site occupation with sodium is already found here at a sodium content of 24%. Assuming that all the K^+ ions occupy the SIII' sites (see above), we can conclude from the linear trend in Figure 5 that the Na^+ population of the SII site begins when the SIII' site occupancy corresponds to a $(\text{Na}^+ + \text{K}^+)$ fractional content of 33%. This number must be contrasted with a threshold value of 63% of Na^+ in the binary system. Thus, our results indicate that the presence of potassium in the SIII site destroys the selective siting of the sodium ions observed in the binary Li,Na-chabazite. While the onset of SII population decreases the rate of the population increase at SIII', both the SII and SIII' site populations continue to increase with increasing sodium content. No site prefer-

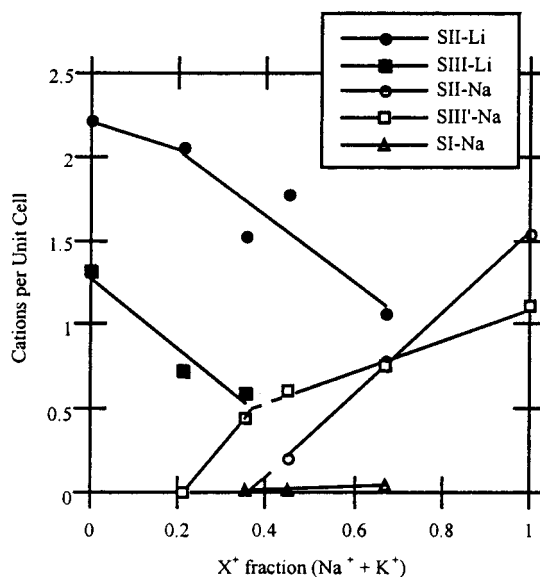


Figure 5. Plot of the sodium and lithium occupancies in the K-containing mixed alkali chabazite as a function of the combined fraction (X^+) of sodium and potassium ions. Filled symbols refer to lithium occupancies, open symbols to sodium occupancies.

ence is observed, although the rate of population increase is greater for sodium at the SII sites than at the SIII' sites, as shown in Figure 5.

The "earlier" Na^+ occupation of the SII site in the Li,Na,K-chabazites has further consequences on the site disorder and distribution in these samples in comparison to the binary system: First of all, it results in a lower population for the disordered SIII'b site. This is understandable, as our previous results on the binary system reveal that population at the SIII'b site is the result of vacancies at the SII site; thus, a reduction in vacancies leads to fewer disordered SIII'b sites. Second, the appearance of two SII-type sites in the ^{23}Na spectra can be rationalized: the early occupation of SII in these samples allows for the possibility that some of these sodium cations have lithium neighbors at the opposite side of the hexagonal prism. The structural distortions to the prism caused by the pairing of these cations can be expected to affect both the chemical shift as well as

the nuclear electric quadrupolar coupling constants, hence resulting in additional disorder not observed in the binary system. On the basis of the spectral parameters of pure Na-chabazite as well as of Na,K-chabazite and of the compositional dependence of the corresponding spectral intensities, it appears plausible that the lower chemical shift associated with SIIa is attributed to a "regular" Na chabazite site, whereas SIIb reflects the site interacting with the lithium ions. This assignment must be considered tentative, however, because the spectral parameters of SIIa and SIIb vary substantially from sample to sample.

Preferential siting of Li at the SII versus the SIII' site in the binary system was previously attributed to the increase in the zeolite lattice constant caused by high sodium occupancies at the SIII' site. The presence of potassium in the system has a similar effect on the lattice; however, the effects are not as dependent on the other cations in the zeolite. In Table 1, the lattice constants for the mixed Li,K- and Na,K-chabazite are listed along with the constants for various compositions in the binary system. In both cases the potassium-containing zeolites have larger lattice constants and unit cell volumes than the binary Na,Li-chabazite. This increase in unit cell volume allows for occupation of the SII site by sodium at lower cation loadings in SIII and also accounts for the presence of a small amount of sodium in the SI site. In the binary system, no sodium occupation of the SI site was observed, even at the largest unit cell volume. These subtle effects associated with the lattice constants are probably driven by small changes in the T-O-T angles. Most likely, the expansion of the lattice caused by the presence of $\approx 20\%$ K⁺

in SIII' results in an expansion of the six-membered ring of the hexagonal prism, allowing for better coordination of the Na⁺ ion.

Conclusions

The introduction of potassium into a mixed lithium-sodium cation system of chabazite destroys the site preferences of sodium through its expansion of the zeolite lattice. The sodium cation will occupy any available site provided the position is unoccupied. In contrast, the presence of potassium has no effect on the lithium site preferences. The inability of potassium to increase Li occupation of the SIII site is disappointing because lithium occupation at this position is important to the gas separation capabilities of chabazite. Nevertheless, the results of the present study show that indirect control over cation site preferences is possible through the introduction of a small amount of a spectator cation that can affect the overall lattice. Judicious selection of cations could lead to the optimal placement of lithium or other cations via direct or indirect effects enabling the fine-tuning of zeolite sorption or catalytic properties.

Acknowledgment. This work was supported by the U.S. Department of Energy under Grant DE-FG03 96ER14672. Financial support was also provided by the Wissenschaftsministerium Nordrhein-Westfalen and by Air Products and Chemicals, Inc. We thank Dr. Tom Gaffney for useful discussions. L.S. thanks the Deutscher Akademischer Austauschdienst (DAAD) for providing travel support.

CM0006392